Table 3 Diagnostic accuracy for the stages of fibrosis by Fibroscan® and ARFI-R (a) Total cases, (b) Viral, (c) Non-viral

	Fibroscan® ($n = 109$)			ARFI-R ($n = 113$)			p value Fibroscan® vs. ARFI-R
	AUC	Cut-off value	LR	AUC	Cut-off value	LR	
(a) Total							
F0 vs. F1–4	0.690	6.2	1.44	0.724	1.02	2.25	0.748
F0–1 vs. F2-4	0.891*	9.1	2.80	0.871*	1.30	2.37	0.512
F0–2 vs. F3–4	0.908*	11.6	3.96	0.890*	1.65	3.86	0.344
F0–3 vs. F4	0.888*	14.3	3.71	0.817*	1.88	3.52	0.908
	Fibroscan® ($n = 59$)			ARFI-R ($n = 59$)			p value Fibroscan® vs. ARFI-R
	AUC	Cut-off value	LR	AUC	Cut-off value	LR	
(b) Viral							
F0 vs. F1–4	NT	NT	NT	NT	NT	NT	NT
F0–1 vs. F2–4	0.887*	11.6	6.93	0.905*	1.40	2.90	0.239
F0–2 vs. F3–4	0.919*	11.6	4.72	0.923*	1.53	4.20	0.229
F0–3 vs. F4	0.924*	17.5	5.56	0.854*	1.88	4.55	0.217
	Fibroscan® ($n = 50$)			ARFI-R ($n = 54$)			p value Fibroscan® vs. ARFI-R
	AUC	Cut-off value	LR	AUC	Cut-off value	LR	
(c) Non-viral							
F0 vs. F1–4	0.677	6.25	1.73	0.730	1.02	2.27	0.724
F0–1 vs. F2–4	0.886*	9.1	3.2	0.842*	1.30	2.48	0.779
F0–2 vs. F3–4	0.882*	11.7	3.27	0.861*	1.45	2.48	0.715
F0–3 vs. F4	0.859*	14.3	3.41	0.793*	2.00	3.34	0.480

AUC area under curve, *LR* likelihood ratio, *NT* not tested

* $p < 0.05$ by χ^2 analysis

stage of fibrosis regardless of whether the cause was viral or non-viral. (Table 3b, c). For patients with non-viral etiology, a subanalysis was conducted to determine the accuracy of elastography measurements in patients with steatohepatitis. This was done because the fibrosis stage in patients with steatohepatitis should be assessed using a different scale (Brunt's classification) [13]. The numbers of patients with stages F0, F1, F2, F3, and F4 were 3, 13, 3, 5, and 7, respectively, by METAVIR classification, and 1, 5, 10, 8, and 7, respectively, by Brunt's classification. The AUROC values for Fibroscan® were 0.820 (F0 vs. F1–4), 0.913 (F0–1 vs. F2–4), 0.904 (F0–2 vs. F3–4), and 0.854 (F0–3 vs. F4) when using the METAVIR classification, and 0.963 (F0 vs. F1–4), 0.898 (F0–1 vs. F2–4), 0.913 (F0–2 vs. F3–4), and 0.854 (F0–3 vs. F4) with Brunt's classification. The AUROC values for ARFI-R were 0.820 (F0 vs. F1–4), 0.846 (F0–1 vs. F2–4), 0.868 (F0–2 vs. F3–4), and 0.738 (F0–3 vs. F4) using the METAVIR classification, and 0.867 (F0 vs. F1–4), 0.797 (F0–1 vs. F2–4), 0.846 (F0–2 vs. F3–4), and 0.738 (F0–3 vs. F4) using Brunt's classification. The accuracy for differentiation between F0 and F1 or higher stages improved when the stage of fibrosis was assessed by Brunt's classification, and thus, both Fibroscan® and ARFI accurately corresponded with fibrosis stage.

Effect of inflammation and steatosis on accuracy of elastography measurement

It has been reported that Fibroscan® data overestimate the pathological stage of fibrosis in samples with severe inflammation [14, 15]. Therefore, we compared the accuracy of elastography measurements according to the inflammatory activity in the liver biopsy specimens. The elastography values increased as the stage of fibrosis increased, regardless of the degree of inflammatory activity (Fig. 6a). As reported previously, among patients with mild fibrosis (F0 and F1), Fibroscan® values were significantly greater in patients with activity of A2–3 versus A0–1. However, these differences were not observed among patients with advanced fibrosis (F2, F3, and F4). The results of ARFI-R were similar to the Fibroscan® results, but no significant differences were observed according to the stage of fibrosis (data not shown). Therefore, the accuracy of these elastography measurements was re-estimated by ROC analysis (Table 4a). For Fibroscan®, the

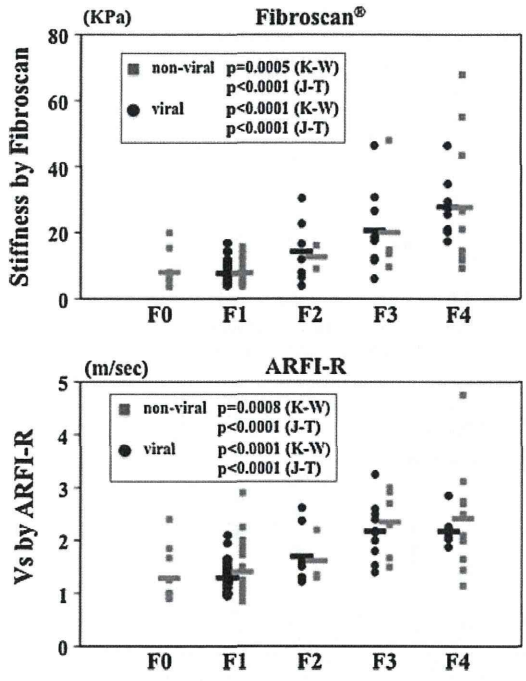

Fig. 5 The accuracy of elastography stratified according to the cause of liver damage. The *black circles* indicate elastography values for patients with viral hepatitis (viral) and the *gray squares* indicate values for patients with other (non-viral) etiologies. The *horizontal lines* indicate the average values for each stage. No patients with viral hepatitis were graded as showing F1. The values of both elastography measurements increased in proportion to the severity of fibrosis (Fibroscan®: (viral) $p < 0.0001$ by Kruskal–Wallis analysis, $p < 0.0001$ by Jonckheere–Terpstra test, (non-viral) $p = 0.0005$ by Kruskal–Wallis analysis, $p < 0.0001$ by Jonckheere–Terpstra test, ARFI-R: (viral) $p < 0.0001$ by Kruskal–Wallis analysis, $p < 0.0001$ by Jonckheere–Terpstra test, (non-viral) $p = 0.0008$ by Kruskal–Wallis analysis, $p < 0.0001$ by Jonckheere–Terpstra test), but there were no significant differences in the elastography values between the viral and non-viral patient groups at the same stages of fibrosis

AUROCs in differentiating F0 vs. F1–4 were 0.802 and 0.511; F0–1 vs. F2–4, the values were 0.899 and 0.861; F0–2 vs. F3–4, the values were 0.936 and 0.867, and F0–3 vs. F4, the values were 0.901 and 0.860 in relation to A0–1 and A2–3, respectively. For ARFI-R, the AUROCs for differentiating the stage of F1 or greater were 0.865 and 0.495; for F2 or greater, the values were 0.889 and 0.839, for F3 or greater, the values were 0.918 and 0.854; and for F4, the values were 0.874 and 0.735. These results indicate that, in patients with mild fibrosis, the accuracy for differentiating the stage of fibrosis decreased with stronger inflammatory activity. In addition, the inflammation only affected differentiation between F0 and F1–4 (Fibroscan® $p = 0.0480$, ARFI-R $p = 0.0082$), but there was no significant difference of diagnostic accuracy in other fibrosis stages by two-way analysis of variance.

Finally, we examined whether elastography measurements were influenced by hepatosteatosis. As shown in Fig. 6b, there were no significant differences between the values for patients with minimal steatosis (S0–1) and those with greater steatosis. The accuracy of elastography measurements was almost identical in the two groups (Table 4b). Moreover, the degree of steatosis did not affect the elastography measurements even when the data were submitted to two-way analysis of variance (data not shown).

Discussion

We herein describe the efficacy of ARFI elastography for the evaluation of liver fibrosis stage in patients with chronic liver damage of various etiologies. The ARFI technique was first introduced clinically to differentiate elastic regions in soft tissues by imaging [16]. Initially, this technology was used to detect tumors in soft tissues such as the liver and mammary gland [17]. Sarvazyan et al. [18] used tissue elastography in two volunteers to measure the velocity of oscillation of a wave generated by ARFI with US. Since then, the technology has evolved and it is now available as a simple machine equipped with US for transient elastography. ARFI technology enabled us to measure real-time liver stiffness during observation of the actual measuring site by B-mode US [21]. In addition to these advantages, tissue elastography with ARFI is very easy to perform and involves simply pushing a button during observation of the site of measurement or ROI. Among many indicators of liver fibrosis, such as elastography, serum fibrosis markers and formulae using various hematologic parameters [19, 20], Fibroscan® has been demonstrated to be the best way. In this study we evaluated the efficacy of ARFI elastography in comparison with that of Fibroscan®.

We attempted to measure both lobes of the liver in this study. The level of stiffness was always higher when we measured the left lobe, though the readings with both elastography methods were highly correlated with the stages of fibrosis. This difference may have been induced by direct pressure of the US probe on the liver when we measured the left lobe. When the right lobe is measured from the intercostal space, the US probe does not directly press on the liver because chest wall exists between US probe and the liver, but in the left lobe, the US probe directly presses on the liver via the abdominal wall. In acute liver damage, it has been reported that liver fibrosis is overestimated with the Fibroscan® method as compared with histology [14, 15]. Similar results were obtained in this study with ARFI, as well as with Fibroscan®; therefore, we excluded elastography values obtained from patients with acute liver damage from most analyses in this study. Moreover, it has been reported that histological

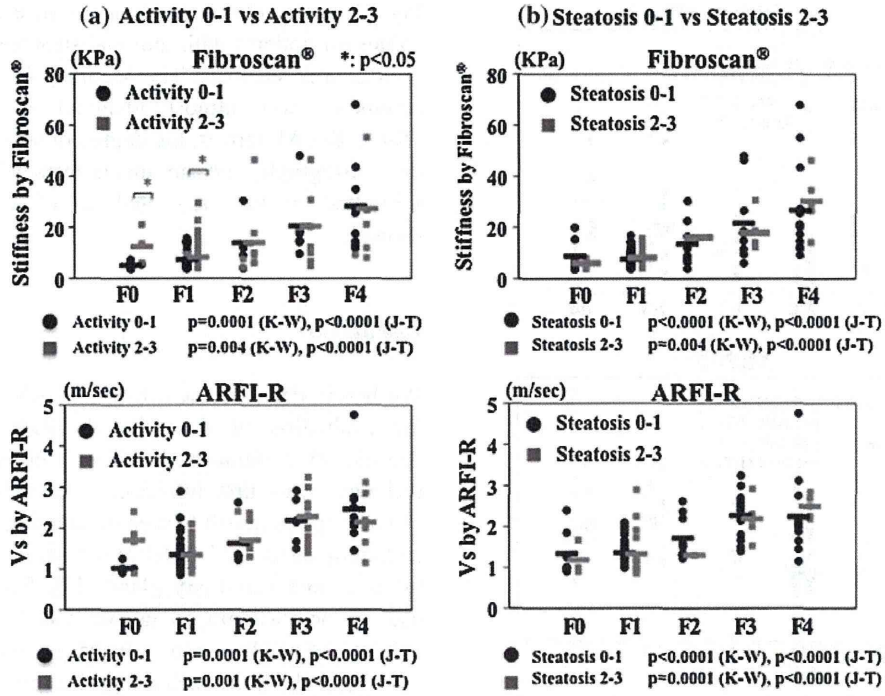

Fig. 6 Differences in elastography values according to the inflammatory activity or degree of steatosis in biopsy specimens. The elastography values increased in proportion to the severity of fibrosis, independently of the grade of inflammatory activity or steatosis. **a** In patients with mild fibrosis, the Fibroscan® values in those with high inflammatory activity (A2–3 *black circles*) were significantly greater than the values in patients with low activity (A0–1 *gray squares*) (F0: 5.1 ± 0.5 for A0–1 vs. 12.4 ± 6.5 for A2–3 $p = 0.0325$, F1: 7.3 ± 4.0 for A0–1 vs. 8.3 ± 3.1 for A2–3 $p = 0.0425$, by Wilcoxon analysis), but there were no significant differences among patients with greater than F2 grade fibrosis. ARFI-R values for patients with high inflammatory activity (A2–3) also tended to be greater than the values for patients with low activity (A0–1), but there were no significant differences at each stage of fibrosis. **b** Values obtained using either Fibroscan® or ARFI-R methods showed no differences between patients with mild steatosis (S0–1 *gray squares*) versus those with more severe steatosis (S2–3 *black circles*)

damage of the liver is uniform in viral hepatitis, which differs, in terms of histological heterogeneity, from findings in other chronic liver diseases such as autoimmune hepatitis and primary biliary cirrhosis. In the present study, measurement values by both ARFI and Fibroscan® increased in parallel with an increase in the stage of fibrosis in patients with viral liver damage as well as in those with non-viral liver damage, but the accuracy of differentiating the stage of fibrosis in patients with non-viral liver damage was slightly lower.

We found that the diagnostic power of differentiation between fibrosis stages with both methods always increased according to the increase in fibrosis stage. These data indicate that the diagnostic power of Fibroscan® and ARFI was almost equal, but the power for differentiating slight fibrosis was weak with both methods. In a meta-analysis of 50 studies with the Fibroscan® method, carried out predominantly in patients with chronic hepatitis C, the mean AUROCs for the diagnosis of significant fibrosis, severe fibrosis, and cirrhosis were 0.84, 0.89, and 0.94, respectively [22]. These findings suggest that transient elastography, performed with either Fibroscan® or ARFI, exhibits higher diagnostic power when fibrosis of the liver is more severe. In the present study, we also analyzed the elastography values by stratifying them according to the grade of inflammation or steatosis in liver biopsy specimens. As reported previously [14, 15], the elastography values in patients with more severe inflammation, (i.e., grade A2 and A3), overestimated the amount of liver fibrosis as compared with the histological findings, but the grade of steatosis did not affect these values. These tendencies were similar with both elastography methods. These factors should be considered when evaluating liver stiffness by tissue elastography.

Liver biopsy is considered the 'gold standard' for diagnosing chronic liver disease, grading necroinflammatory activity, and staging liver fibrosis. However, sampling error can lead to the underestimation of liver fibrosis, especially when biopsy specimens are small or fragmented [3, 4]. In the present study, the Fibroscan® values (20.5 kPa) and ARFI-R values (2.2 m/s) in patients with F3 stage fibrosis were higher than those described in previous reports [23–25]. The Fibroscan® value in our previous report was also lower (13.85 kPa) [8]. It may be difficult to

Table 4 Accuracy of elastography determined by receiver operating characteristic (ROC) analysis stratified by inflammatory activity (a) and steatosis (b) of the liver biopsy specimen (* $p < 0.05$ by χ^2 analysis)

	Fibroscan®						ARFI-R					
	Activity 0–1 ($n = 57$)			Activity 2–3 ($n = 52$)			Activity 0–1 ($n = 59$)			Activity 2–3 ($n = 54$)		
	AUC	Cut-off value	LR	AUC	Cut-off value	LR	AUC	Cut-off value	LR	AUC	Cut-off value	LR
(a) Inflammatory activity												
F0 vs. F1–4	0.802	6.3	3.60	0.511	6.2	1.13	0.865*	1.05	5.19	0.495	1.00	1.31
F0–1 vs. F2–4	0.899*	9.1	4.28	0.861*	11.6	3.95	0.889*	1.30	3.01	0.839*	1.51	2.69
F0–2 vs. F3–4	0.936*	11.7	4.69	0.867*	11.6	3.33	0.918*	1.67	5.25	0.854*	1.80	3.89
F0–3 vs. F4	0.901*	17.5	8.05	0.860*	20.3	8.06	0.874*	1.88	4.32	0.735*	2.00	3.07
	Fibroscan®						ARFI-R					
	Steatosis 0–1 ($n = 80$)			Steatosis 2–3 ($n = 29$)			Steatosis 0–1 ($n = 82$)			Steatosis 2–3 ($n = 31$)		
	AUC	Cut-off value	LR	AUC	Cut-off value	LR	AUC	Cut-off value	LR	AUC	Cut-off value	LR
(b) Steatosis												
F0 vs. F1–4	0.647	6.3	1.65	0.793	6.7	2.16	0.726	1.02	2.21	0.741	1.02	2.33
F0–1 vs. F2–4	0.867*	9.1	2.61	0.957*	12.3	8.50	0.854*	1.35	2.22	0.900*	1.30	3.80
F0–2 vs. F3–4	0.894*	11.6	4.06	0.933*	12.3	6.00	0.870*	1.65	3.96	0.920*	1.53	4.00
F0–3 vs. F4	0.872*	17.5	5.08	0.935*	18.8	9.20	0.782*	1.88	3.49	0.896*	2.19	6.25

differentiate accurately between F3 and F4 by observing specimens obtained by liver needle biopsy, and pathological findings could sometimes underestimate the actual fibrosis. The cut-off values obtained by ROC analysis for differentiating F0–3 from F4 were 14.3 kPa and 1.88 m/s, respectively. These data were similar to those described in previous reports [23, 24, 26]. Liver biopsy is not suitable for repeated evaluations because it is invasive and can cause major complications (0.3–0.5%), including death (0.03–0.1%) [5]. Moreover, liver fibrosis is a sequential and/or continuous process, and the staging of liver fibrosis should be evaluated frequently. In contrast to liver biopsy, transient elastography is non-invasive and can be repeated many times in the same patient. This feature is very useful clinically. Masuzaki et al. [27] prospectively studied the efficacy of Fibroscan® in predicting HCC development in patients with chronic hepatitis C, and demonstrated encouraging results. Thus, transient elastography provides a new procedure to assess and predict some of the clinical signs of chronic liver disease.

In the present study, we compared values of ARFI to the values with the Fibroscan® method. ARFI was superior in terms of its convenience because it is equipped with US. In this study, ARFI could be performed on all patients, while Fibroscan® failed for 4 patients because of the presence of thick subcutaneous fat tissue and/or liver atrophy. These drawbacks have been pointed out previously [28]. Moreover, the accuracy of diagnosing the stages of fibrosis by ARFI is similar to that with the Fibroscan® method and is considered to be satisfactory, although differentiation of the existence of slight fibrosis was deemed to be insufficient. Recently Lupsor et al. [11] reported preliminary results for a study comparing the ARFI and Fibroscan® methods in patients with chronic hepatitis C. They found that both ARFI and Fibroscan® data were strongly correlated with the stage of fibrosis, and Fibroscan® was better for predictions of earlier stages. However, our prospective study incorporated a percutaneous liver biopsy taken at the same time as the elastography measurements, and we did not find that the Fibroscan® method was superior in the earlier stages.

In conclusion, we evaluated the utility of transient elastography by ARFI for the diagnosis of liver fibrosis and found that the ARFI data correlated significantly with fibrosis staging. Although there are several issues that should be considered carefully in the future (such as inflammation), we conclude that transient elastography with ARFI method, as well as Fibroscan®, is a very simple, non-invasive, and useful procedure in the field of hepatology.

References

1. Manning DS, Afdhal NH. Diagnosis and quantitation of fibrosis. Gastroenterology. 2008;134:1670–81.
2. Sherlock S. Aspiration liver biopsy, technique and diagnostic application. Lancet. 1945;ii:397.

3. Regev A, Berho M, Jeffers LJ, Milikowski C, Molina EG, Pyrsopoulos NT, et al. Sampling error and intraobserver variation in liver biopsy in patients with chronic HCV infection. Am J Gastroenterol. 2002;97:2614–8.
4. Bedossa P, Dargere D, Paradis V. Sampling variability of liver fibrosis in chronic hepatitis C. Hepatology. 2003;38:1449–57.
5. Dienstag JL. The role of liver biopsy in chronic hepatitis C. Hepatology. 2002;36:S152–60.
6. Poniachik J, Bernstein DE, Reddy KR, Jeffers LJ, Coelho-Little ME, Civantos F, et al. The role of laparoscopy in the diagnosis of cirrhosis. Gastrointest Endosc. 1996;43:568–71.
7. Sandrin L, Fourquet B, Hasquenoph JM, Yon S, Fournier C, Mal F, et al. Transient elastography: a new noninvasive method for assessment of hepatic fibrosis. Ultrasound Med Biol. 2003;29:1705–13.
8. Saito H, Tada S, Nakamoto N, Kitamura K, Horikawa H, Kurita S, et al. Efficacy of non-invasive elastometry on staging of hepatic fibrosis. Hepatol Res. 2004;29:97–103.
9. Fahey BJ, Nightingale KR, Nelson RC, Palmeri ML, Trahey GE. Acoustic radiation force impulse imaging of the abdomen: demonstration of feasibility and utility. Ultrasound Med Biol. 2005;31:1185–98.
10. Palmeri ML, Wang MH, Dahl JJ, Frinkley KD, Nightingale KR. Quantifying hepatic shear modulus in vivo using acoustic radiation force. Ultrasound Med Biol. 2008;34:546–58.
11. Lupsor M, Badea R, Stefanescu H, Sparchez Z, Branda H, Serban A, et al. Performance of a new elastographic method (ARFI technology) compared to unidimensional transient elastography in the noninvasive assessment of chronic hepatitis C. Preliminary results. J Gastrointestin Liver Dis. 2009;18:303–10.
12. The French METAVIR Cooperative Study Group. Intraobserver and interobserver variations in liver biopsy interpretation in patients with chronic hepatitis C. Hepatology. 1994;20:15–20.
13. Brunt EM. Nonalcoholic steatohepatitis: definition and pathology. Semin Liver Dis. 2001;21:3–16.
14. Sagir A, Erhardt A, Schmitt M, Häussinger D. Transient elastography is unreliable for detection of cirrhosis in patients with acute liver damage. Hepatology. 2008;47:592–5.
15. Arena U, Vizzutti F, Corti G, Ambu S, Stasi C, Bresci S, et al. Acute viral hepatitis increases liver stiffness values measured by transient elastography. Hepatology. 2008;47:380–4.
16. Nightingale RK, Soo MS, Nightingale R, Trahey G. Acoustic radiation force impulse imaging: in vivo demonstration of clinical feasibility. Ultrasound Med Biol. 2002;28:227–35.
17. Palmeri ML, Frinkley KD, Zhai L, Gottfried M, Bentley RC, Ludwig K. Acoustic radiation force impulse (ARFI) imaging of the gastrointestinal tract. Ultrason Imaging. 2005;27:75–88.
18. Sarvazyan AP, Rudenko OV, Swanson SD, Fowlkes JB, Emelianov SY. Shear wave elasticity imaging: a new ultrasonic technology of medical diagnostics. Ultrasound Med Biol. 1998;24:1419–35.
19. Wai CT, Greenson JK, Fontana RJ, Kalbfleisch JD, Marrero JA, Conjeevaram HS, et al. A simple noninvasive index can predict both significant fibrosis and cirrhosis in patients with chronic hepatitis C. Hepatology. 2003;38:518–26.
20. Imbert-Bismut F, Ratziu V, Pieroni L, Charlotte F, Benhamou Y, Poynard T, et al. Biochemical markers of liver fibrosis in patients with hepatitis C virus infection: a prospective study. Lancet. 2001;357:1069–75.
21. Talwalkar JA, Kurtz DM, Schoenleber SJ, West CP, Montori VM. Ultrasound-based transient elastography for the detection of hepatic fibrosis: systematic review and meta-analysis. Clin Gastroenterol Hepatol. 2007;5:1214–20.
22. Friedrich-Rust M, Ong MF, Martens S, Sarrazin C, Bojunga J, Zeuzem S, et al. Performance of transient elastography for the staging of liver fibrosis: a meta-analysis. Gastroenterology. 2008;134:960–74.
23. Foucher J, Chanteloup E, Vergniol J, Caste'ra L, Le Bail B, Adhoute X et al. Diagnosis of cirrhosis by transient elastography (FibroScan): a prospective study. Gut. 2006;55:403–8.
24. Kim KM, Choi W-B, Park SH, Yu E, Lee SG, Lim Y-S, et al. Diagnosis of hepatic steatosis and fibrosis by transient elastography in asymptomatic healthy individuals: a prospective study of living related potential liver donors. J Gastroenterol. 2007;42:382–8.
25. Iijima H. The usefulness of non-invasive diagnosis of liver fibrosis using acoustic radiation force impulse. Kanzo. 2010;51:54–5.
26. Obara N, Ueno Y, Fukushima K, Nakagome Y, Kakazu E, Kimura O, et al. Transient elastography for measurement of liver stiffness measurement can detect early significant hepatic fibrosis in Japanese patients with viral and nonviral liver diseases. J Gastroenterol. 2008;43:720–8.
27. Masuzaki R, Tateishi R, Yoshida H, Goto E, Sato T, Ohki T, et al. Prospective risk assessment for hepatocellular carcinoma development in patients with chronic hepatitis C by transient elastography. Hepatology. 2009;49:1954–61.
28. Kettaneh A, Marcellin P, Douvin C, Poupon R, Ziol M, Beaugrand M, et al. Features associated with success rate and performance of FibroScan measurements for the diagnosis of cirrhosis in HCV patients: a prospective study of 935 patients. J Hepatol. 2007;46:628–34.

Clinica Chimica Acta 412 (2011) 1767–1772

Contents lists available at ScienceDirect

Clinica Chimica Acta

journal homepage: www.elsevier.com/locate/clinchim

LecT-Hepa: A triplex lectin–antibody sandwich immunoassay for estimating the progression dynamics of liver fibrosis assisted by a bedside clinical chemistry analyzer and an automated pretreatment machine

Atsushi Kuno[a], Yuzuru Ikehara[a], Yasuhito Tanaka[b], Kozue Saito[a], Kiyoaki Ito[c], Chikayuki Tsuruno[d], Shinya Nagai[d], Youichi Takahama[d], Masashi Mizokami[c], Jun Hirabayashi[a], Hisashi Narimatsu[a,*]

[a] Research Center for Medical Glycoscience (RCMG), National Institute of Advanced Industrial Science and Technology (AIST), 1-1-1 Umezono, Tsukuba, Ibaraki 305–8568, Japan
[b] Department of Virology & Liver Unit, Nagoya City University Graduate School of Medical Sciences, Kawasumi, Mizuho, Nagoya 467–8601, Japan
[c] The Research Center for Hepatitis and Immunology, National Center for Global Health and Medicine, Ichikawa, Japan
[d] Product Development Div. 2, Sysmex Corporation, 4-4-4 Takatsukadai, Nishi-ku, Kobe 651–2271, Japan

ARTICLE INFO

Article history:
Received 22 April 2011
Received in revised form 23 May 2011
Accepted 23 May 2011
Available online 30 May 2011

Keywords:
Alpha1-acid glycoprotein
Biomarker
Glycoprotein
Hepatitis C virus
Liver fibrosis
Sandwich immunoassay

ABSTRACT

Background: A quantitative analysis of glyco-alteration in serum glycoproteins provides glyco-parameters for estimating the progression of liver fibrosis. In the analysis of glycans, a manual pretreatment process for clinical specimens leads to a complicated manipulation and loss-of-clinical implementation of the assay.
Method: We evaluated an automated triplex lectin–antibody sandwich immunoassay assisted by an automated protein purification system (ED-01) and a bedside clinical chemistry analyzer (HISCL) for the acquisition of two glyco-parameters (AOL/DSA and MAL/DSA) derived from a fibrosis-related glyco-alteration of serum alpha1-acid glycoprotein (AGP).
Results: We adjusted the auto-machines with their accuracy set to CV <5.0% (ED-01) and <1.0% (HISCL). AGP samples were enriched from 275 serum specimens. Two glyco-parameters obtained by HISCL showed a linear correlation with that from a reported assay ($R>0.90$). The formula for monitoring fibrosis (LecT-Hepa) was given by a combination of the glyco-parameters. This correlated with the fibrosis stage from biopsy ($R=0.68$) and diagnosed severe fibrosis and cirrhosis. It was superior to that of FIB-4 index.
Conclusions: We automated a multilectin-assisted immunoassay with an order of magnitude reduction of operation time without any loss-of-accuracy. LecT-Hepa is a reliable method to assess fibrosis-dynamics from moderate fibrosis to cirrhosis.

1. Introduction

Secreted proteins are practically glycosylated in the endoplasmic reticulum and the Golgi apparatus. Since the features of glycosylation depend on the extent of cell differentiation and the state of the cell, i.e., the origin of a tissue, its developmental stage and the presence of malignancy, blood glycoproteins consist of a mixture of heterogeneous molecules derived from many sources [1,2]. Thus, glycoproteins that exhibit disease-associated glyco-alteration and are present in serum have the potential to act as biomarkers for the diagnosis of a target disease. Numerous glycoproteins have been studied to date as candidate glyco-biomarkers accompanied by rapid advances in glycomics technologies. Such glyco-markers have attracted a great deal of attention in the "discovery phase" of clinical applications [3].

Hepatitis B and C viral (HBV, HCV) infections are prevalent health problems, affecting 350 million and 170 million people, respectively, worldwide. This situation is becoming worse because chronic hepatitis (CH) caused by HCV infection will result in an increase in the incidence of liver cirrhosis (LC) accompanied by an irreversible progression of fibrosis. As about 80% of LC patients (the worst fibrosis stage) have contracted hepatocellular carcinoma (HCC) within the past 10 y, >90% of HCC cases in Japan have originated from chronic hepatitis caused by HCV (81%) or HBV (13%) infection. It is evident that the best way of monitoring the progression of hepatitis is to establish an accurate serological method for the quantitative evaluation of fibrosis, as well as the early detection of HCC. Consequently, a large variety of noninvasive methods have been developed [4], including FibroScan [5], which physically analyzes the progression of liver fibrosis based on transient elastography, and FibroTest [6,7] and Hepascore [8], which are serological tests employing a narrow and complex algorithm derived using a patient's age, sex and biochemical markers. Recently, FIB-4, which uses the patient's age, aspartate aminotransferase (AST), alanine aminotransferase (ALT) and platelet count, has been developed as a simple, inexpensive and accurate fibrosis index in patients with HCV [9–11].

Detecting hepatic disease-associated glyco-markers for clinical applications has been a continuous challenge since the early 1990s,

* Corresponding author. Tel.: +81 29 861 3200.
E-mail address: h.narimatsu@aist.go.jp (H. Narimatsu).

0009-8981/$ – see front matter © 2011 Elsevier B.V. All rights reserved.
doi:10.1016/j.cca.2011.05.028

because increased fucosylation on complex-type *N*-glycans has been frequently detected in glycoproteins from patients with HCC and LC [12–14]. Of all the alpha-fetoprotein (AFP) glycoforms, more than 30% have been found to react to a fucose-binding lectin, *Lens culinaris* agglutinin. This fraction, designated as AFP-L3, was approved by the US FDA in 2005 for the diagnosis and prognosis of HCC [13]. Recently, an immunoassay system for AFP-L3 was automated by combining affinity electrophoresis and recent microfluidics technology [15]. Other challenges have been proposed for diagnosing liver cirrhosis and HCC using recent technology for glycan analysis [16–20]. Callewaert et al. have developed a series of glycan-based liver disease tests [16,17,21,22] based on a capillary electrophoresis-based DNA sequencer. They found that the ratio between two disease-specific glycans helps in the accurate monitoring of liver fibrosis and the diagnosis of compensated cirrhosis and HCC in cirrhosis patients [21]. This system has a big advantage in terms of simplicity over other highly reliable serological tests, such as FibroTest, which measure the α2-macroglobulin/apolipoprotein A-I ratio using two different analyzers. This system had been developed further in terms of a higher throughput and rapid glycan profiling using microfluidics for its clinical implementation [22]. However, this system requires a three-hour manual pretreatment process, i.e., protein denaturation, release of *N*-glycans, desialylation and labeling.

In the context of the development of a fibrosis-related glycoprotein marker, an acute-phase protein alpha1-acid glycoprotein (AGP) is thought to be one of the best candidates, because it is a well-characterized glycoprotein with five highly branched complex-type *N*-glycans, whose alteration (e.g., fucosylation and desialylation) occurs during the progression of liver fibrosis and carcinogenesis [12]. Using these properties, an increased degree of fucosylation was detected in cirrhosis patients using a fucose-binding lectin (AAL)-antibody sandwich ELISA employing an automated analyzer [23]. The detection of asialo-AGP using lactosamine-recognition lectin RCA120 has been reported as an alternative method for detecting cirrhosis, and a rapid immunochromatographic strip test has been developed [24–26]. Recently, we further optimized this useful lectin set for monitoring fibrosis using an antibody-assisted lectin profiling system (ALP) [27]. A multiplex sandwich immunoassay using a 43-lectin microarray detected many other aspects of glyco-alteration of AGP, resulting in the selection of two lectins (*Maackia amurensis* lectin (MAL) and *Aspergillus oryzae* lectin (AOL)) and *Datura stramonium* lectin (DSA) as a fibrosis indicator and a signal normalizer [28]. The resulting two glyco-parameters (AOL/DSA and MAL/DSA) gave a definitive criterion formula that distinguished well between LC and CH patients with a diagnostic accuracy of >90%. We confirmed that the use of this lectin set was statistically superior to previously selected lectins, including AAL and RCA120. This triplex-sandwich immunoassay employing DSA/MAL/AOL lectins and an anti-AGP antibody is expected to be further simplified to be able to be performed by bedside clinical chemistry analyzers. In this study, we evaluated the clinical implementation of our triplex assay. We adopted an automated protein purification machine, the Enrichment Device (ED-01; GP BioSciences Ltd., Yokohama, Japan) (shown in the schematic diagram in Fig. 1) to immunoprecipitate AGP from serum in a rapid, high-throughput and reproducible manner. To enable simple manipulation and a high diffusion rate of the assay, we shifted the detection system from the lectin microarray to a fully automated immunoassay analyzer (HISCL-2000i). The resulting criterion formula for detecting liver fibrosis (LecT-Hepa) was compared with the following fibrosis markers and indices: FIB-4 [9–11], hyaluronic acid (HA) [29,30] and Type IV collagen (IV-Col) [31].

2. Materials and methods

2.1. Patient samples, biochemical parameters and indices

The 175 patients with chronic hepatitis C used as the case subjects were identical to those used in our previous report [28]. The control

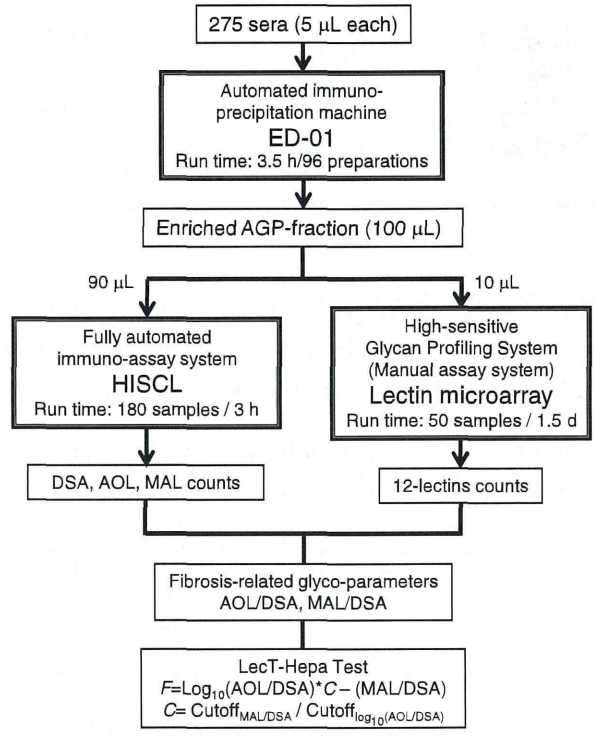

Fig. 1. Schematic diagram for evaluating the progression dynamics of liver fibrosis.

subjects were population-based samples from 100 randomly selected healthy volunteers aged 22–77 y. All sera were collected at Nagoya City University Hospital. The institutional ethics committees at Nagoya City University Hospital and National Institute of Advanced Industrial Science and Technology (AIST) approved this study, and informed consent for the use of their clinical specimens was obtained from all individuals before collection at Nagoya City University Hospital and AIST. Fibrosis was graded for 125 patients according to the Histologic Activity Index using biopsy or surgical specimens. For all patients, the following biological parameters were determined at the time of blood collection: aspartate aminotransferase (AST), alanine aminotransferase (ALT) and platelet count. Serum HA and IV-Col were measured using Latex Agglutination Turbidimetric Immunoassay (SRL Inc, Tokyo, Japan). The FIB-4 index was calculated as follows: [age (years) × AST (U/l)]/[platelets (10^9/l) × ALT (U/l)$^{1/2}$] [9].

2.2. Immunoprecipitation of AGP from serum using an automated protein purification system

We employed an automated protein purification system (ED-01; GP BioSciences Ltd.) to immunoprecipitate AGP from a serum. The working reagents and protocol were followed as listed in a previous report [28], but were optimized for the machine. In brief, all the sera were diluted in a ratio of 1:10 with PBS containing 0.2% SDS, and then heated at 95 °C for 20 min. The resulting solution (50 μl) was mixed with 10 μl of Triton X-100 in TBS (TBSTx) and injected into a 96-well SUMILON microtiter plate (Sumitomo Bakelite Co. Ltd., Tokyo, Japan). The plate and working reagents, which included the biotinylated anti-AGP antibody (50 ng/μl), the streptavidin-immobilized magnetic bead, the washing buffer (1% TBSTx) and the elution buffer (TBS containing 0.2% SDS), were set into the designated position in the machine. After setting the materials, the AGPs (110 μl) were automatically purified (96 samples for 3.5 h).

2.3. A rapid lectin–antibody sandwich immunoassay using HISCL

Fibrosis-specific glyco-alteration of AGP was qualified from simultaneous measurements of the lectin–antibody sandwich immunoassays using three lectins (DSA, MAL and AOL). In principle, the glycan part of the AGP was captured by the lectin immobilized on the magnetic beads, and the captured AGP was then quantified by an anti-human AGP mouse monoclonal antibody probe that was cross-linked to an alkaline phosphatase (ALP-αAGP). The assay manipulation was fully automated using a chemiluminescence enzyme immunoassay machine (HISCL-2000i; Sysmex Co., Kobe, Japan). Four reagent packs, i.e., an AGP-DSA detection reagent pack, an AGP-MAL detection reagent pack, an AGP-AOL detection reagent pack and a chemiluminescence substrate reagent pack, were placed into position in the HISCL machine. Each detection reagent pack comprised three reagents: a reaction buffer solution (R1), a lectin-coated magnetic beads solution (R2) and an ALP-αAGP solution (R3). The chemiluminescence substrate reagent pack contained a CDP-Star substrate solution (R4) and a stopping solution (R5). A representative procedure for the DSA-antibody sandwich assay is described as follows. An aliquot of the AGP-enriched solution (30 μl) was diluted to 60 μl with the R1 solution, and then mixed with the R2 solution (30 μl). After the binding reaction, the R3 reagent (100 μl) was added to the reaction solution. The resulting conjugates were magnetically separated from any unbound AGPs and ALP-αAGP, and substantially mixed with R4 (50 μl) and R5 (100 μl). The chemiluminescent intensity was acquired over a period of 17 min in the operation described above. The reaction chamber was kept at a temperature of 42 °C during the HISCL measurements. The MAL-AGP and AOL-AGP sandwich assays were performed using the same procedure.

2.4. Glycan profiling of AGP using a lectin microarray

The enriched AGPs were subjected to an antibody-overlay lectin microarray [27,28,32] to validate the glycan profiles of the serum AGPs. An aliquot of the purified proteins (4 μl) was diluted to 60 μl with PBS containing 1% Triton X-100 (PBSTx); this was then applied to a LecChip™ (GP BioSciences Ltd.), which included three spots of 45 lectins in each of seven reaction wells. After incubation for 12 h, an excess blocker glycoprotein (2 μl of nonlabeled human serum IgG (10 mg/ml)) was added to the chip and incubated for 30 min. The reaction solution was then discarded, and the chip was washed 3 times with PBSTx. A volume of 60 μl of 50 ng of a biotinylated antibody solution in PBSTx was then applied to the chip, and incubated for 1 h. After three washes with PBSTx, 60 μl of 100 ng of a Cy3-labeled streptavidin (GE Healthcare Buckinghamshire, UK) solution in PBSTx was added and incubated for 30 min. The chip was rinsed with PBSTx and scanned using an evanescent-field fluorescence scanner (GlycoStation™ Reader1200; GP BioSciences Ltd.). We analyzed all the data using the Array Pro Analyzer software package, version 4.5 (Media Cybernetics, Inc., Bethesda, MD). The net intensity value for each spot was calculated by subtracting the background value from the signal intensity values of the 3 spots. We elected to scan data under appropriate gain conditions, which provided the intensities of all positive spots as <40,000. The relative intensities of the positive lectins were determined from their ratio to the fluorescent intensity of the internal-standard lectin DSA.

2.5. Statistics

We performed statistical analyses using the Dr. SPSS II software package for Windows (SPSS Co., Tokyo, Japan), Origin version 8.0 software package for Windows (LightStone Co., Tokyo, Japan) and Excel 2007 for Windows to compare the diagnostic value of the LecT-Hepa test with other serological fibrosis markers or indices. The correlation of the biomarkers with liver fibrosis was estimated from the samples obtained from 110 patients from the correlation coefficient (R) and the *P*-values were calculated using a nonparametric test (the Mann–Whitney *U*-test). To assess the classification efficiencies of various markers for detecting significant fibrosis, severe fibrosis and cirrhosis [33], the receiver operating characteristic (ROC) curve analysis was also carried out to determine the area under the curve (AUC) values. We used the cutoff values obtained from Youden's index [34] to classify the patients. The diagnostic accuracy was expressed as the diagnostic specificity, sensitivity, positive predictive value (PPV), negative predictive value (NPV), overall accuracy and AUC [35].

3. Results and discussion

3.1. Optimization of an automated protein purification machine for AGP enrichment

We first optimized an automated protein purification machine (ED-01) from GP BioSciences to enrich the serum AGP, which was subjected to a rapid and automated triplex lectin–antibody sandwich immunoassay using HISCL to acquire the fibrosis-related glyco-parameters (Fig. 1). To achieve this, we considered the significant difference in the reaction conditions between the automatic assay and a previous manual assay using a lectin microarray. In brief, in the case of HISCL, the binding reaction between the lectin-coated magnetic beads and the analyte AGP must occur within a period of <5 min. In the case of the lectin microarray, the analyte was incubated with lectins immobilized on a glass slide for >12 h. For these reasons, the AGP was enriched from 5 μl of serum for HISCL, which was an order of magnitude larger than that of the lectin microarray (0.5 μl of serum used). The amount of the capturing biotinylated antibody for HISCL was additionally increased to 1 μg per sample, which was five times larger than that of the lectin microarray. These modifications resulted in us obtaining a sufficient amount of AGPs to complete a triplex sandwich assay using HISCL (data not shown). Next, we examined the accuracy of the auto-machine. Sera from a normal healthy volunteer and a patient with HCC were randomly divided into 44 and 3 wells on a 96-well microtiter plate, respectively. PBSTx as a blank was added into a well at the same time. The dispensed plate was then subjected to automatic immunoprecipitation. After a 3.5 h automatic immunoprecipitation period, each enriched AGP was quantitatively compared using the signal intensity of the DSA lectin acquired by the antibody-overlay lectin microarray analysis, which was used as an internal standard because the intensity correlated well with the amount of AGP [28]. From the result from the normal healthy volunteer, the intensity of DSA was averaged to 30,304 with high reproducibility (SD = 1506, CV = 4.97%) (Supplementary Table 1). The quality of the enriched AGP was maintained at a high level to distinguish the glycosylation alteration of AGPs accompanied by the progression of liver fibrosis, i.e., distinction of glycan profiles between the normal healthy volunteer and the patient with HCC using lectin microarray, as reported previously (Supplementary Fig. 1 and Ref. [28]). Collectively, automation of the pretreatment process was optimized to provide the enriched AGP for the next automated sandwich assay (Fig. 1).

3.2. Measurement of a triplex lectin–antibody immunoassay using HISCL

HISCL is an automated sandwich immunoassay system based on the luminescence-assisted detection principle employing a capturing antibody immobilized on magnetic beads and a detection antibody conjugated with alkaline phosphatase. As the HISCL measurement completes within 17 min for clinical implementation, each antigen–antibody interaction reaction must be rapid and strong enough to detect the antigen within the operation time. On the other hand, the glycan (glycoprotein)–lectin interaction is significantly weaker than the antigen–antibody interaction. To overcome this problem in terms of its clinical usefulness, we adapted "high density" lectin magnetic beads. Because our target glycoprotein AGP bore five highly branched

N-glycans, an obviously strong cluster effect was expected to occur from the interaction between the immobilized lectin and the glycans of AGP. In addition, a high abundance of AGP in the sera (0.5–1.0 mg/ml) made it possible to undergo an immediate reaction on the immobilized lectin from the high concentration of the analyte AGP. Keeping in mind these considerations, we evaluated a triplex lectin–antibody immunoassay for the serum AGP using HISCL. The AGPs were enriched from pooled human sera for quality control (Nissui Pharmaceutical Co., Tokyo, Japan) and pooled plasma for the HCV patients. The former was used to measure the lectin–antibody sandwich assays with MAL and DSA, and the latter was used for the assay with AOL. The simultaneous repeatability of each assay was evaluated by performing 10 independent experiments. The resulting coefficient of variation (CV) was in the range 0.6%–1.0%. The sensitivity was evaluated by performing the assay on a serial dilution of the enriched AGP solution from a dilution ratio in the range $1/2^5$ to $1/2^0$ to generate a standard curve. As a negative control, the assay was carried out in the absence of AGP. The background luminescence value (9277 for DSA, 3839 for MAL and 93078 for AOL) was subtracted from the values obtained from all the samples. A linear regression revealed the linear range of detection (R^2>0.99), at least within the above dilution ratio (Fig. 2a–c). The linear range was sufficient to quantify the glyco-alteration of AGP, since the quantification of the glyco-alteration in the previous lectin microarray analysis was performed using AGP concentrations within the range of the five serial dilutions. Taken together, the rapid and automated system performed a triplex lectin–antibody sandwich immunoassay for detecting glyco-alteration of AGP with high reliability.

3.3. Similarities of the 2 glyco-parameters obtained using HISCL to those obtained using lectin microarray

Next, we examined whether the 2 fibrosis-related glyco-parameters (AOL/DSA and MAL/DSA) established using the lectin microarray were represented by the HISCL measurements (see schematic diagram in Fig. 1). All the sera used in this study were pretreated in the automachine ED-01, as described above, and each enrichment fraction (100 μl) was then divided into a 90 μl portion for HISCL and a 10 μl portion for the lectin microarray. We performed a triplex lectin–antibody sandwich assay using both systems with sera from 275 specimens (175 HCV patients and 100 healthy volunteers), and we then determined the two glyco-parameters. As shown in the resulting scatter plots, the upper limit of detection for HISCL was higher than that of the lectin microarray (Fig. 2d and e). According to the best linear curve with its correlation coefficient and the coefficient of determination (R^2 = 0.91 for AOL/DSA and 0.82 for MAL/DSA), we confirmed that the use of the rapid and automated assay system could acquire the two glyco-parameters.

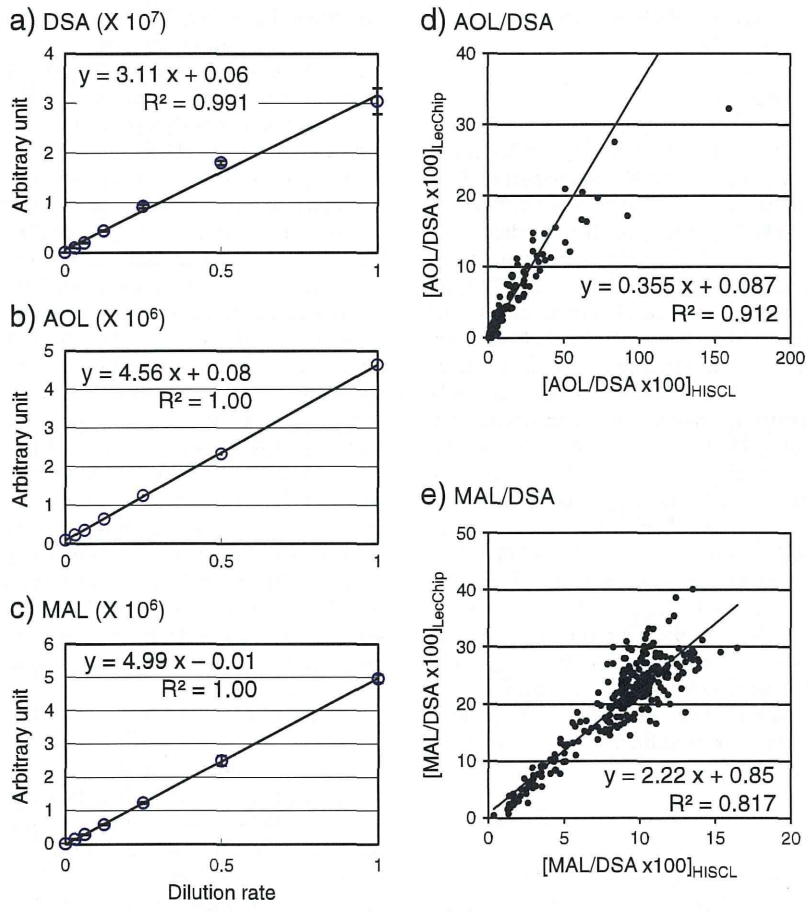

Fig. 2. Rapid operation for obtaining two glyco-parameters (AOL/DSA, MAL/DSA). Standard curves for the quantification of AGPs specifically binding to: (a) DSA, (b) AOL and (c) MAL lectins using an automated lectin–antibody sandwich immunoassay employing HISCL. Each data point represents the mean of triplicate independent experiments with the error bars showing the mean ± standard deviation. Each glyco-parameter (d) AOL/DSA and (e) MAL/DSA was determined using 275 different serum samples for both HISCL and a manual assay employing a lectin microarray. The graphs show scatter plots, and the best linear curve with its correlation coefficient was calculated using the Excel 2007 software package (Microsoft). The plots were limited (<50 for HISCL) in the calculation of the correlation coefficient for AOL/DSA.

3.4. Definition of a criterion formula for estimating the progression of liver fibrosis

To assess the correlation of the two obtained glyco-parameters with the progression of fibrosis, we analyzed the data from HISCL measurements on 125 HCV patients (F0–F1, 26.4% (33 patients); F2, 25.6% (32 patients); F3, 24% (30 patients); and F4, 23.2% (29 patients)). As shown on the left-hand side of Supplementary Fig. 2, the MAL/DSA values gradually decreased with the progression of fibrosis, and the Pearson's correlation coefficient was R = −0.67. On the other hand, the AOL/DSA values increased exponentially. Indeed, the Pearson's correlation coefficient of Log_{10}(AOL/DSA) was R = 0.68, which is higher than that of AOL/DSA (R = 0.51). Both parameters fitted for the quantification of the progression of fibrosis from F2 to F4. Next, we examined the AUC to characterize the diagnostic accuracy of cirrhosis (F4). For the prediction of cirrhosis, the AUC, diagnostic sensitivity, diagnostic specificity and the cutoff value of AOL/DSA were 0.89 (95% CI 0.82–0.97), 89%, 81% and 4.15, respectively (right-hand side of Supplementary Fig. 2). MAL/DSA could detect cirrhosis with an AUC = 0.85 (95% CI 0.83–0.97), a diagnostic sensitivity of 85%, a diagnostic specificity of 88% and a cutoff value of 5.31. These values suggest that AOL/DSA tended to favor sensitive detection, whereas the MAL/DSA functions suppressed the pseudo positive rate. We developed the following criterion formula, named the "LecT-Hepa Test", to enhance the diagnostic accuracy by combining both glyco-parameters:

$$F = \mathrm{Log}_{10}[\mathrm{AOL}/\mathrm{DSA}]^{*}C-[\mathrm{MAL}/\mathrm{DSA}],\ \text{and}$$

$$C = \mathrm{Cutoff}_{\mathrm{MAL}/\mathrm{DSA}} / \mathrm{Cutoff}_{\mathrm{log10(AOL}/\mathrm{DSA)}}$$

where Cutoff_x is the cutoff value for distinguishing liver cirrhosis in the 125 patients by glyco-parameter X. In this study, we calculated a value of $C = 5.31/\mathrm{Log}_{10}4.15 = 8.6$. The LecT-Hepa Test correlated well with the progression of fibrosis (R = 0.68). In addition, we tested the accuracy of LecT-Hepa for the diagnosis of liver cirrhosis using a validation data set from another 88 patients (liver cirrhosis, $n = 45$; chronic hepatitis, $n = 43$) used in a previous report [28]. The LecT-Hepa detected liver cirrhosis with a diagnostic sensitivity of 91% and a diagnostic specificity of 91%, whereas AOL/DSA and MAL/DSA had a diagnostic sensitivity of 91% and a diagnostic specificity of 89%, and a diagnostic sensitivity of 77% and a diagnostic specificity of 96%, respectively. Furthermore, the pseudo positive rates of MAL/DSA, AOL/DSA and LecT-Hepa targeted from 100 normal healthy volunteers were 0%, 11% and 2%, respectively. These results indicate that the use of the rapid and automated assay system to acquire a fibrosis-related formula (LecT-Hepa) comprising the two glyco-parameters was valid.

3.5. Comparison of serological fibrosis biomarkers and indices

Finally, we compared the diagnostic accuracy of each lectin value at each stage of fibrosis, i.e., significant fibrosis (F2, F3 and F4), severe fibrosis (F3 and F4) and cirrhosis (F4), between LecT-Hepa and other fibrosis markers. HA and IV-Col were selected as comparable fibrosis markers acquired by the single biomarker measurement, as well as FIB-4, which is well known as an inexpensive and accurate fibrosis index of four parameters obtained in general blood tests [9–11]. In this examination, the objective specimens were limited to the sera from 110 patients (F0, 1 = 32, F2 = 32, F3 = 28 and F4 = 18) because of their availability for all parameters, i.e., age, platelet count, AST, ALT, HA, IV-Col, AOL/DSA and MAL/DSA. The resulting serum levels and the distribution of fibrosis markers and indices are shown in Supplementary Table 2 and Fig. 3. On comparing the correlation coefficient between these data, we found that LecT-Hepa (R = 0.68) was the best for estimating fibrosis dynamics. Although all the tests including LecT-Hepa increased exponentially with the progression of fibrosis, LecT-Hepa particularly distinguished between F2, F3 and F4 patients. The observation

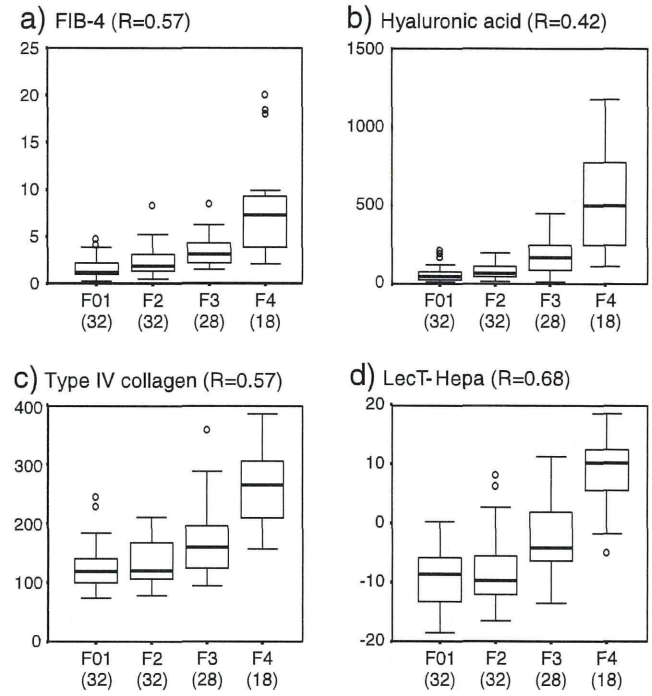

Fig. 3. Correlation of four fibrosis markers with the progression of liver fibrosis. Box–whisker plots according to the Histologic Activity Index show the 75th and 25th percentiles (the top and bottom of the box, respectively), the median (line through the middle of the box) and the 95th and 5th percentiles (the top and bottom of the whiskers, respectively), as well as the R, Pearson's correlation coefficient between the fibrosis stage from biopsy and the fibrosis markers.

was supported by the following estimation using a nonparametric test (the Mann–Whitney *U*-test) and ROC investigation (Table 1). Because the ROC curves were compiled to estimate their cutoff values using the data set from 110 patients (F0, 1, 2, 3 = 92, F4 = 18), the number of patients with fibrosis stage F4 was not sufficient to compare the diagnostic values for detecting cirrhosis. For this reason, we used an additional 19 patients with LC determined using ultrasonography (coarse liver architecture, nodular liver surface and blunt liver edges) and evidence of hypersplenism (splenomegaly in the ultrasonography) in 175 HCV patients. As a result, LecT-Hepa could still detect liver cirrhosis with high diagnostic accuracy (diagnostic sensitivity of 89%, diagnostic specificity of 86%, overall accuracy of 87%, PPV of 72% and NPV of 95%), which is superior to the values of FIB-4 (diagnostic sensitivity of 84%, diagnostic specificity of 83%, overall accuracy of 83%, PPV of 66% and NPV of 93%) and HA (diagnostic sensitivity of 95%, diagnostic specificity of 74%, overall accuracy of 80%, PPV of 59% and NPV of 97%). Interestingly, the false diagnosis cases with LecT-Hepa were not necessarily identical to those with FIB-4 (Supplementary Table 3). This suggests that a combination of LecT-Hepa and FIB-4 would be effective.

4. Conclusions

We developed a triplex lectin–antibody immunoassay using a bedside clinical chemistry analyzer. This allows a marked reduction in operation time from 12 h to <30 min per triplex assay of a sample, resulting in its clinical usefulness. The reliability was secured by the full automation of the pretreatment process. The diagnostic score of LecT-Hepa was superior to that of other serological indices and markers. Consequently, LecT-Hepa evolved reliably to assess the dynamics of fibrosis from moderate fibrosis to cirrhosis. Further validation tests are underway.

Supplementary materials related to this article can be found online at doi:10.1016/j.cca.2011.05.028.